ORIGINAL RESEARCH

Modified active disturbance rejection control scheme for systems with time delay

Josu Jugo[1] 🔘 | **Ander Elejaga**[1] | **Pablo Echevarria**[2]

[1]Electricity and Electronics Department, University of the Basque Country UPV/EHU, Campus Leioa, Spain

[2]Helmholtz-Zentrum Berlin, Berlin, Germany

Correspondence
Josu Jugo, Electricity and Electronics Department, University of the Basque Country UPV/EHU, Campus Leioa 48940, Spain.
Email: josu.jugo@ehu.eus

Abstract
Active disturbance rejection control (ADRC) has been gaining attention in recent years and has shown its performance in multiple applications including non-linear ones, without the need of accurate models. Despite the good results of this technique, time delay can deteriorate the performance of ADRC, limiting its application. Here, the effect of time delay on the stability of a linear ADRC is analysed, using an alternative mathematical description, and a new effective design technique, based on a modified ADRC scheme, is proposed to overcome the delay effect while maintaining the disturbance rejection properties of the ADRC. An experimental example is discussed considering a system with low damped mechanical resonances, showing good results using the proposed technique.

1 | INTRODUCTION

Active disturbance rejection control (ADRC) has gained relevance in recent years, due to its growing successful application [1–4] and the recent research increasing its theoretical background [1, 5–9]. Sometimes presented as an evolution of the classical proportional integral derivative control (PID) [1], the ADRC technique is based in four fundamental elements: a simple differential equation as a transient trajectory generator, a noise-tolerant tracking differentiator, the non-linear control laws and the use of the concept of total disturbance estimation and rejection.

One of the keys of the ADRC control technique is the extended state observer (ESO), which estimates the external disturbances and considers the internal dynamics as another disturbance. The plant is reduced to a simple chained integrator form by using a control law, in which model-based design methods can be applied. Furthermore, feedback of the extended state, consisting of the internal dynamics and the external disturbance, allows the reduction of the total disturbance. This way the desired system dynamics is obtained simultaneously with the disturbance reduction. In addition, the ADRC control effort is usually lower than that required with other control techniques.

However, as with other control techniques, ADRC control has practical limitations. An important limitation of feedback control arises from the presence of time delay, which reduces the stability range. The delay introduces a phase that is linearly dependent with the frequency, limiting the gain at higher frequencies in order to maintain the stability. This effect is especially relevant in the presence of poorly damped resonances, as high gains with high phase shift are difficult to manage with feedback control. The delay limits the disturbance reduction bandwidth that can be obtained with the conventional ADRC control scheme. An example of a system with this problem is the control of microphonics in superconducting RF cavities used in particle accelerators, where distortion reduction is critical to keep the cavity resonance around the nominal value [10]. Several works deal with the time delay effect by mean of ADRC-based schemes and several methods have been proposed [11–16]. One possibility proposed by Han is to ignore the time-delay and design the ADRC for dynamics without time-delay, but this technique limits the performance obtained. Another possibility is the use of a Padé approximation, increasing the system order, but it is only valid for small time-delays [1, 13, 16]. To take in account the time-delay, in [11, 12] it was suggested to delay the control signal by the same amount before it enters

the ESO. In [14], a generalized proportional integral (PI) control based on Smith's predictor, and the ADRC philosophy, is proposed for a class of delayed-input non-linear mechanical systems. In [15], tracking control of uncertain time-delayed systems is proposed, which is implemented in a predictor scheme for time-delay compensation. In [16], a two-degree-of-freedom (2DOF) control structure is proposed for unstable time-delayed systems. In general, these methods improve stability in the presence of time-delay but reduce the disturbance rejection effect. More recently, probabilistic robustness-based ADRC design has also been applied to systems with delay [17].

Disturbance reduction is a key control objective in systems with low damped resonances for many applications, such as control of microphonics in superconducting cavities for particle accelerators, [2–4]. ADRC is a good candidate for these applications, but the effect of relatively small time-delays can be crucial due to the stability problems introduced by this delay, which limits its application and effective disturbance rejection. This relatively small delay can be easily introduced by actuators.

This work studies the effect of the delay in the stability of a linear ADRC (LADRC) control system. The result of this study is a novel strategy based on LADRC to increase the stability in the presence of time delay, obtaining an improvement in disturbance rejection. The main contributions are:

- A mathematical description of LADRC that facilitates the analysis of stability and the effect of the time delay.
- The analysis of the time-delay effect using LADRC, based on the mathematical description presented.
- A new modified LADRC control scheme (MLADRC), valid for increasing the delay stability margin.

First, in Section 2, the stability analysis of a delayed LADRC system is performed, after rewriting the basic scheme following a similar way to the one in [12]. The system description obtained allows the definition of the MLADRC algorithm, presented in Section 3, which facilitates the stability analysis and adds a new control element, increasing the designer's freedom. The design of this control element for stabilizing the closed-loop system in the presence of time-delay is discussed, using loop shaping as design technique. The resulting scheme allows to improve the stability in the presence of time-delay, maintaining as much as possible the so-called matching condition and, therefore, improving the disturbance reduction. An experimental application example involving mechanical resonances is used to discuss in detail the full procedure, which shows good results and improved disturbance rejection.

2 | STABILITY ANALYSIS OF LINEAR ADRC SYSTEMS WITH TIME-DELAY

In this section, the analysis of an LADRC is carried out, following the description proposed in [18] and including the effect of an input time-delay.

Consider a linear system described in the Laplace domain by the expression:

$$Y(s) = e^{-\tau_s} P(s) \left(U(s) + \xi_1(s) \right) + \xi_2(s) \tag{1}$$

where $P(s)$ is a transfer function representing the system dynamics, $\xi_{1,2}(s)$ are the external disturbances of the system and τ is the input time-delay.

In the original ADRC description, the system model is not a requirement, this being one of the powerful characteristics of this control approach. The only information needed is the relative order of $P(s)$, that is, $p := n-m$, and its high-frequency gain $b = b_m/a_n$, where n and m are the order of the denominator and numerator of the transfer function $P(s)$, respectively, and a_n and b_m are the coefficients of the highest degrees.

Ignoring for the moment the delay to simplify the development, the controlled plant is described by the following model:

$$y^{(p)}(t) = bu(t) + f(t) \tag{2}$$

where $f(t)$ is a combination of the unknown plant dynamics and the external plant disturbance, which is called the generalized disturbance and assumed to be unknown in the ADRC design framework.

Following this design scheme, the central idea is to estimate the unknown generalized disturbance ($f(t)$). To do so, a Luenberger-type extended linear observer (ESO) is defined. Let

$$z_1 = y, z_2 = \dot{y}, \ldots, z_p = y^{(p-1)}, z_{p+1} = f \tag{3}$$

Assume that f is differentiable and let $\dot{f} = h$. Then, (2) can be written as

$$\begin{cases} \dot{z} = A_e z + B_e u + E_e h \\ y = C_e z \end{cases}$$

where $z = [z_1, z_2 \ldots, z_p, z_{p+1}]^T$ and

$$A_e = \begin{bmatrix} 0 & 1 & 0 & \ldots & 0 \\ 0 & 0 & 1 & \ldots & 0 \\ \vdots & \vdots & \vdots & \ddots & \vdots \\ 0 & 0 & 0 & \ldots & 1 \\ 0 & 0 & 0 & \ldots & 0 \end{bmatrix}_{(p+1)\times(p+1)} \tag{4}$$

$$B_e = \begin{bmatrix} 0 & 0 & \ldots & b & 0 \end{bmatrix}^T_{(p+1)\times1}$$
$$E_e = \begin{bmatrix} 0 & 0 & \ldots & 0 & 1 \end{bmatrix}^T_{(p+1)\times1}$$
$$C_e = \begin{bmatrix} 1 & 0 & 0 & \ldots & 0 \end{bmatrix}^T_{(p+1)\times1}$$

A full-order Luenberger state observer can be designed as follows:

$$\begin{cases} \dot{\hat{z}} = A_e \hat{z} + B_e u + L_o \left(y - \hat{y} \right) \\ \hat{y} = C_e \hat{z} \end{cases}$$
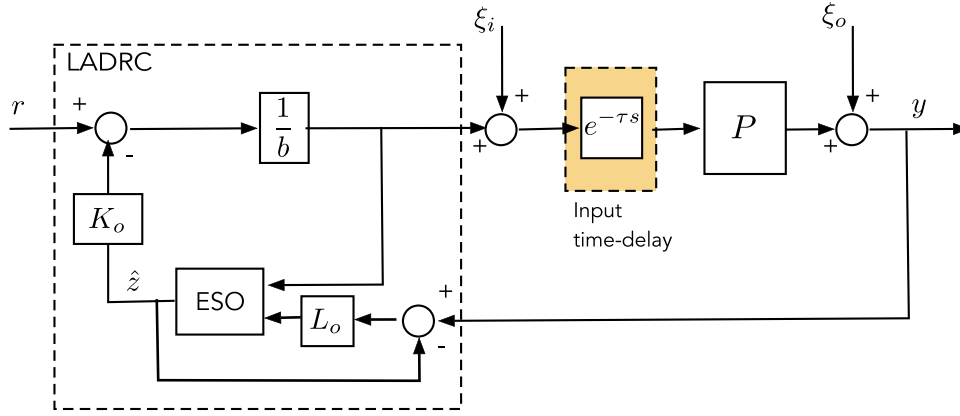
FIGURE 1 Structure of the classical LADRC, including the plant an input delay.

where L_o is the observer gain vector $L_o = [\beta_1 \; \beta_2 \; ... \; \beta_p \; \beta_{p+1}]^T$.

The gain vector L_o is a designer's tool, which defines the bandwidth of the observer ω_o and delimits the frequency range of the disturbances to be considered and must be selected to ensure that $A_e - L_oC$ is asymptotically stable. The values $\hat{z}_1(t), ..., \hat{z}_p(t)$ estimate $y(t)$, $\hat{y}(t)$, and its derivatives, and $\hat{z}_{p+1}(t)$ estimates the generalized disturbance $f(t)$. This estimated disturbance is the key control element in ADRC control, since it can be used to force the system to follow the desired dynamics, while the external disturbance is minimized, when the stability is maintained.

In this work, the reference tracking is not considered necessary, since the main objective is the disturbance reduction. For this reason, the use of a tracking differentiator (TD) is not considered hereinafter, simplifying the discussion. Under these conditions, the control can be defined:

$$ u(t) = \frac{r - K_o' \left[\hat{z}_1(t), ..., \hat{z}_p(t) \right]^T - \hat{z}_{p+1}(t)}{b} $$

where K_o' is the controller gain for the pth-order integral plant and r the reference signal. This second gain vector is another designer's tool, which defines the controller bandwidth ω_c, [18]. Defining $K_o = [K_o', 1]$, the LADRC can be described:

$$
\begin{cases}
\dot{\hat{z}}(t) & = A_e\hat{z}(t) + B_e u(t) + L_o \left(y(t) - C_e\hat{z}(t) \right) \\
& = (A_e - L_oC_e)\hat{z}(t) + B_e u(t) + L_o y(t) \\
u(t) & = \frac{r - K_o\left[\hat{z}_1(t),...,\hat{z}_{p+1}(t)\right]^T}{b}
\end{cases}
\tag{5}
$$

In this classical description, the LADRC is a "general" control structure which is independent of the original plant model, except for the relative order p of the model and the high-frequency gain b. Moreover, a LADRC can be tuned with two parameters (ω_c and ω_o), and, thus, is easy to understand by practical control engineers [17]. The scheme of this system can be observed in Figure 1, including the plant an input time delay. The designer does not need to know the detailed structure and

the parameters of the model, so it is quite similar to PID control which has a fixed control structure that is independent of the plant models.

2.1 | Alternative system description

To facilitate the analysis, the system shown in Figure 1 can be restructured as in Figure 2 following a similar way to the one proposed in [11], and a generalized ESO H_{eso} can be defined [19].

From this scheme and (5), this generalized ESO (GESO) can be described by the following state-space representation:

$$
\begin{cases}
\dot{\hat{z}}(t) = A_o\hat{z}(t) + B_o \begin{bmatrix} r(t) \\ y(t) \end{bmatrix} \\
y_{o(t)} = K_o\hat{z}(t) \\
A_o = A_e - L_oC_e - \frac{K_o}{b}B_e \\
B_o = \left[\frac{B_e}{b} \; L_o \right]
\end{cases}
\tag{6}
$$

where K_o defines the desired dynamics, which is now included in the GESO description. Note that (6) is equivalent to (5).

Following a similar description of the state-space realization (6) using the Laplace Transform presented in [19], the GESO can be described as follows:

$$
\hat{Z}(s) = A_o\hat{Z}(s) + \frac{B_e}{b}R(s) + L_oY(s)
$$
$$
Y_o(s) = K_o\hat{Z}
\tag{7}
$$

Deleting the intermediate variable $\hat{Z}(s)$, the GESO output $Y_o(s)$ is:

$$
Y_o(s) = K_o \left(sI_{(p+1)\times(p+1)} - A_o \right)^{-1} \frac{B_e}{b}R
$$
$$
+ K_o \left(sI_{(p+1)\times(p+1)} - A_o \right)^{-1} L_oY(s)
\tag{8}
$$

which can be rewritten by a two-degree-of-freedom conventional feedback structure as shown in Figure 3:
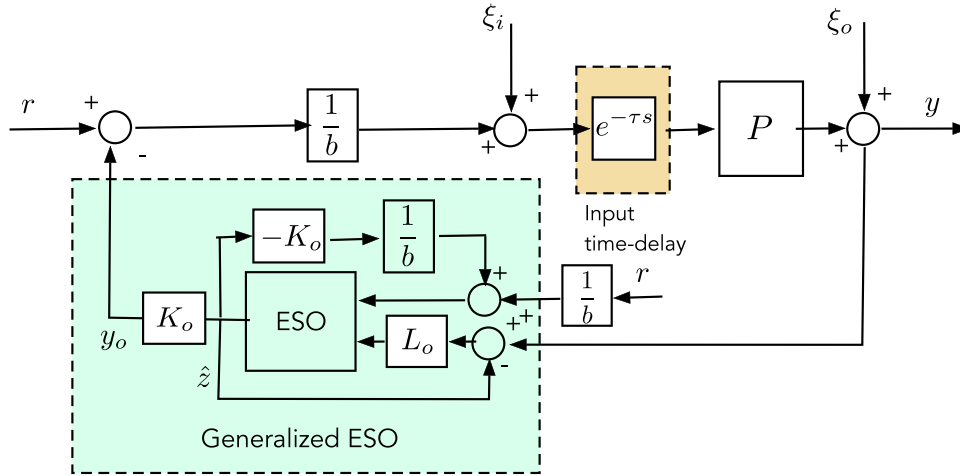
FIGURE 2 Alternative description of the classical LADRC structure, which eases the system analysis.
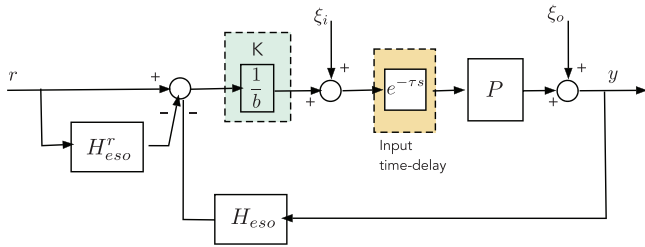

FIGURE 3 Equivalent system description of the classical LADRC using transfer functions.

$$Y_o(s) = H_{eso}(s) Y(s) + H_{eso}^r(s) R(s)$$
$$H_{eso} = K_o \left(sI_{(p+1)\times(p+1)} - A_o \right)^{-1} L_o$$
$$H_{eso}^r = K_o \left(sI_{(p+1)\times(p+1)} - A_o \right)^{-1} \frac{B_e}{b} \quad (9)$$

Note that the denominator of $H_{eso}(s)$ and $H_{eso}^r(s)$ transfer functions is the same.

This description facilitates the stability analysis of the LADRC system. Using the transfer functions in (9), the closed loop characteristic equation derived from Figure 3 can be written:

$$1 + e^{-\tau s} K H_{eso}(s) P(s) = 0 \quad (10)$$

The roots of (10) are the poles of the closed loop transfer function and gives the stability of the system which can be studied as function of the direct-loop gain K, for a particular time delay τ. Note that $K = \frac{1}{b}$ is the nominal value that satisfies the matching condition, since this description is valid for any time delay, including $\tau = 0$.

When τ is not 0, the analytical solution of equation (10) is not easy, since the number of roots is infinity. However, frequency domain methods, such as the Nyquist criterion, are valid in this case [11, 20]. By obtaining the Nyquist diagram (or Bode diagram for open loop stable systems) from the expression $e^{-\tau s} K H_{eso}(s) P(s)$, the stability of the system can be analysed by the Nyquist criterion and the delay stability margin can be easily obtained.

As a straightforward result, if the original system is open-loop stable, for any delay τ a sufficiently low K makes the closed-loop system stable [20]. However, if this K value is lower than $1/b$ the matching condition is not fulfilled, and the disturbance reduction is diminished.

The equivalent description of Figure 3 is only valid for analysis and not as an alternative implementation scheme since numerical issues may arise.

Now, consider the next expression:

$$H_{eso}(s) = H_{eso}^e(s) + H_{eso}^f(s) \quad (11)$$

being

$$H_{eso}^e(s) = \left[K_o', 0 \right] \left(sI_{(p+1)\times(p+1)} - A_o \right)^{-1} L_o$$
$$H_{eso}^f(s) = [0, \dots, 0, 1] \left(sI_{(p+1)\times(p+1)} - A_o \right)^{-1} L_o \quad (12)$$

where H_{eso}^f defines the feedback loop dependent on $f(t)$, that is, the extended state which estimates the system dynamic and the external disturbances, and H_{eso}^e depends on the rest of the state vector. Note that the denominator of the transfer functions $H_{eso}^e(s)$ and $H_{eso}^f(s)$ are equal and have a pole in the origin, since the matching condition is satisfied by definition of matrix A_o. The use of these transfer functions must be done carefully to avoid numerical problems, since both have the same denominator.

Using the relation (11), the feedback loop in Figure 3 can be separated into two loops, which can be analysed independently.
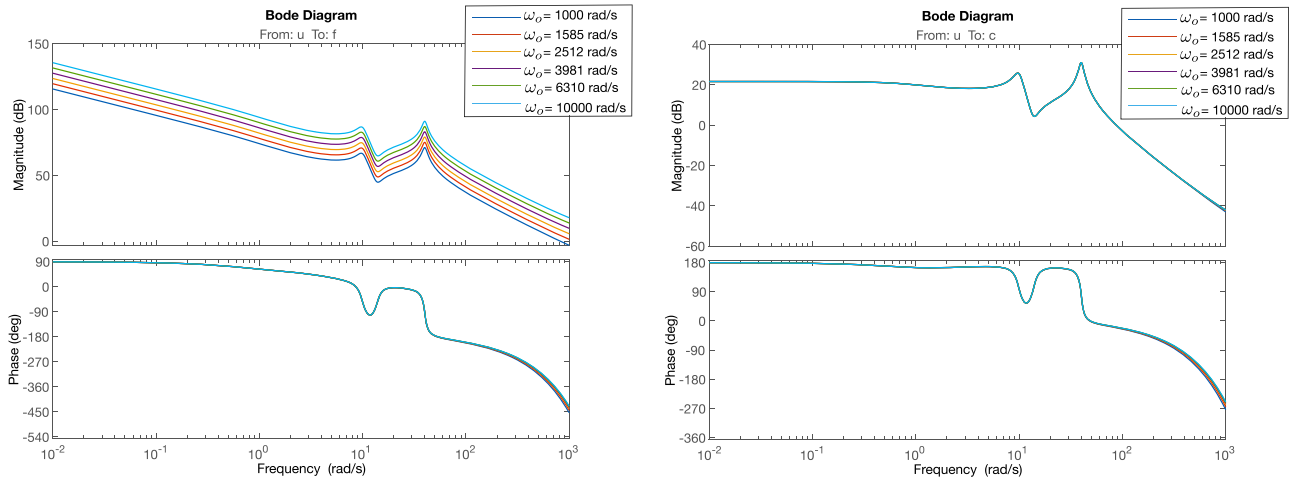
FIGURE 4 Open loop Bode diagrams with $\omega_c = 5$ rad/s and $\tau = 0.005$ s, for different values of the observer bandwidth ω_o. Left: $e^{-\tau s}H_{eso}^f P$, Right: $e^{-\tau s}H_{eso}^c P$. The phase increases linearly with τ.

To illustrate the effect of each loop, an example with two mechanical resonances is considered:

$$P(s) = \frac{1.4}{(s+1)} + g_0 + g_1$$

$$g_0 = \frac{\omega_0^2}{(s^2 + 2\delta_0\omega_0 s + \omega_0^2)} \qquad (13)$$

$$g_1 = \frac{\omega_1^2}{(s^2 + 2\delta_1\omega_1 s + \omega_1^2)}$$

with $\omega_0 = 10$ rad/s, $\delta_0 = 0.1$, $\omega_1 = 40$ rad/s, $\delta_1 = 0.05$ and a constant delay $\tau = 0.005$ s. Those values have been chosen for defining a system with low relative stability.

For this system, several LADRC controllers (first order) have been defined from (6), using different values of the ESO observer bandwidth ω_o (two poles in $-\omega_o$) for obtaining L_o, and of the controller bandwidth ω_c (one pole in $-\omega_c$) for computing K_o. First, the controller bandwidth $\omega_c = 5$ rad/s is maintained constant and different values of the ESO observer bandwidth ω_o are used, obtaining the open-loop transfer functions $e^{-\tau s}KH_{eso}^f(s)P(s)$ and $e^{-\tau s}KH_{eso}^c(s)P(s)$ using (12), for the analysis of its influence on the system stability. Figure 4 shows the Bode diagrams for both transfer functions with different values of ω_o.

Similarly, several LADRC controllers (again first order) has been defined keeping constant $\omega_o = 1000$ rad/s for different values of the LADRC control bandwidth ω_c. Figure 5 shows the Bode diagrams for the open-loop transfer functions $e^{-\tau s}KH_{eso}^f(s)P(s)$ and $e^{-\tau s}KH_{eso}^c(s)P(s)$, for such systems.

Observing Figures 4 and 5, the effect of reducing or increasing the observer bandwidth is closely related to the change of the gain value in the disturbance estimation loop ($H_{eso}^f(s)P(s))$), that is, K.

Other relevant conclusion, observed in all the figures, is the evident effect of the delay $\tau = 0.005$ s on the stability of the LADRC system. This effect is especially important for the loop with feedback of the estimated disturbance. The high

gain responsible of the disturbance reduction makes the system unstable with relatively low time delay, since the delay increases the phase lag proportionally with the frequency. In this case, following the Nyquist criterion for stable open-loop systems, the system becomes unstable if the system amplitude is higher than 0 db at frequencies with a phase lag higher than -180 degrees. The figures show that the mentioned phase limit is always gained due to the delay effect and, then, all cases have a maximum system gain that guarantees the stability. This maximum allowable gain limits the capacity of distortion reduction.

This example shows that, comparing both feedback loops, the disturbance estimation loop ($H_{eso}^f(s)P(s)$) is the dominant one, that is, its open-loop gain is much larger and can be considered the main control effect of the LADRC scheme.

From the previous analysis, it is clear that the expression (10) facilitates the stability analysis of the LADRC controller, especially in the presence of time delay. Taking into account these results and with the aim of increasing the design flexibility, a new scheme based on the LADRC controller is proposed in the next section.

3 | MODIFIED LADRC CONTROLLER

The original design procedure for an ADRC controller is based in two steps. First, the observer gains L_o are selected considering the canonical system (4) and the desired estimation bandwidth ω_o and, second, a controller gain K_o' is selected to define the desired control bandwidth ω_c. The controller and estimation bandwidth are selected to not interfere with each other.

In this section, a modified LADRC (MLADRC) controller, which follows other design procedure, is presented. This MLADRC is based on a novel GESO scheme, which has some similarities with the proposed one in [20], and it has been derived from the previous discussion and observing the transfer functions (9).
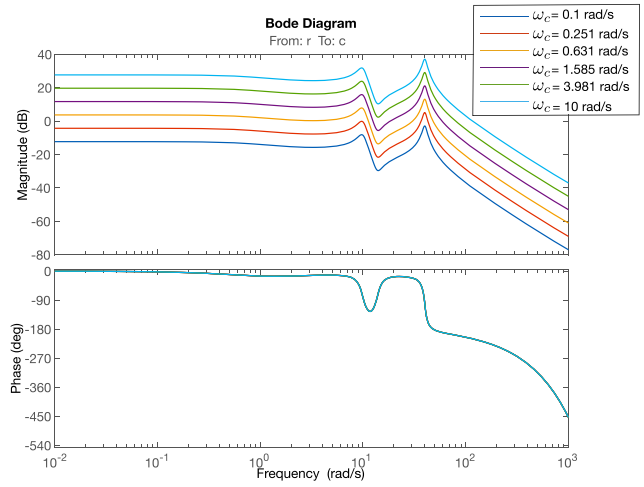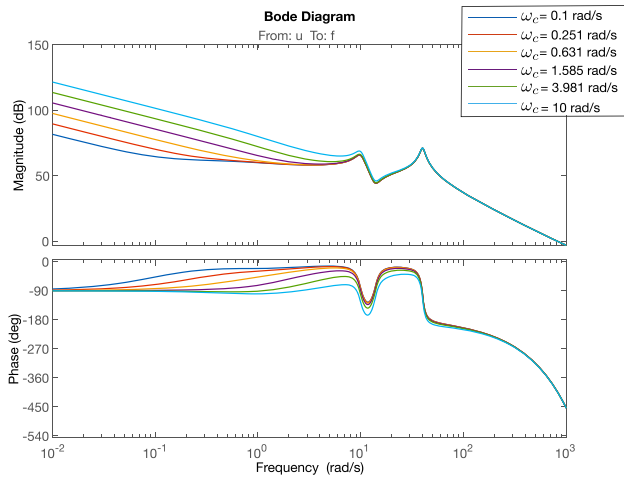
FIGURE 5 Open loop Bode diagrams with $\omega_0 = 1000$ rad/s and $\tau = 0.005$ s, for different values of the control bandwidth ω_c. Left: $e^{-\tau s} H_{eso}^f P$, Right: $e^{-\tau s} H_{eso}^c P$. The phase increases linearly with τ.

First, the new GESO structure is presented, which can be described by the following state space representation:

$$
\begin{cases}
\dot{\hat{z}}(t) = A_o \hat{z}(t) + B_o \begin{bmatrix} r(t) \\ y(t) \end{bmatrix} \\
y_o(t) = K_o \hat{z}(t) \\
A_o = A_e - L_o C_e - \dfrac{K_o}{b} B_e \\
B_o = \begin{bmatrix} \dfrac{B_e}{b} & L_o \end{bmatrix}
\end{cases}
\tag{14}
$$

being $K_o = [K_o', 1]$, $\hat{z} = [\hat{z}_1, \hat{z}_2 \cdots, \hat{z}_p, \hat{z}_{p+1}]^T$ and

$$
A_e = \begin{bmatrix}
0 & 1 & 0 & \dots & 0 \\
0 & 0 & 1 & \dots & 0 \\
\vdots & \vdots & \vdots & \ddots & \vdots \\
0 & 0 & 0 & \dots & 1 \\
0 & 0 & 0 & \dots & 0
\end{bmatrix}_{(p+1)\times(p+1)}
\tag{15}
$$

$$
B_e = \begin{bmatrix} 0 & 0 & \cdots & b & 0 \end{bmatrix}^T_{(p+1)\times 1}
$$
$$
C_e = \begin{bmatrix} 1 & 0 & 0 & \cdots & 0 \end{bmatrix}^T_{(p+1)\times 1}
$$

The design parameters are selected as follows:

- The controller gains K_o' are calculated to get the desired closed-loop dynamics by solving the pole placement problem defined by ω_c. The vector of desired poles for the controller is $[\omega_c, \omega_c, \cdots, \omega_c]_{1xp}$. Using this gain vector, an auxiliary ESO matrix is defined, $A_e - \dfrac{[K_o', 0]}{b} B$.
- Using the auxiliary matrix, the observer is designed for a chosen observer bandwidth, ω_o. The vector of desired poles for the observer is $[\omega_o, \omega_o, \dots, \omega_o]_{1x(p+1)}$. With a valid L_o vector, the resulting GESO dynamics will be stable since the
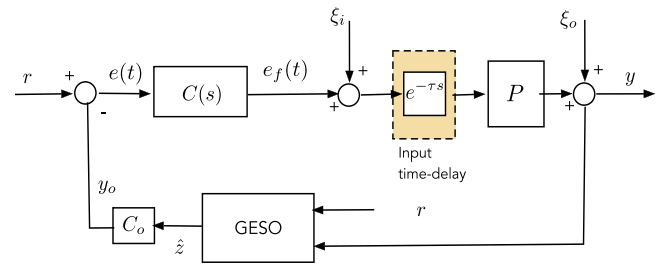
interaction between the controller and observer bandwidth is included in the observer design.

- Define the definitive GESO matrix $A_o = A_e - L_o C_e - \dfrac{K_o}{b} B_e$. This matrix assures the fulfilment of the matching condition in the GESO.

The GESO, as shown in Figure 6, uses as inputs the reference $r(t)$ and the output of the plant to be controlled. One of the main novelties if this GESO is the direct introduction of the effect of the disturbance estimation feedback in matrix A_o, as can be observed in the definition of A_o in Equation (15). This change isolates the matching condition with respect to the direct loop gain (originally $1/b$). So, by changing the direct loop gain, the GESO maintains the matching condition.

In addition, this scheme allows the use of two possible alternatives by defining $C_o = K_o$ or $C_o = [0, \dots, 1]$:

- In the first case, the full feedback loop (H_{eso}) is used, similarly to the typical LADRC scheme.
- In the second case, the feedback is obtained only by means of estimating the total disturbance $f(t)$ (H_{eso}^f). This is a new proposal, but taking into account the nature of the total disturbance and the analysis of the example presented in the previous section, the expected dynamics obtained from the
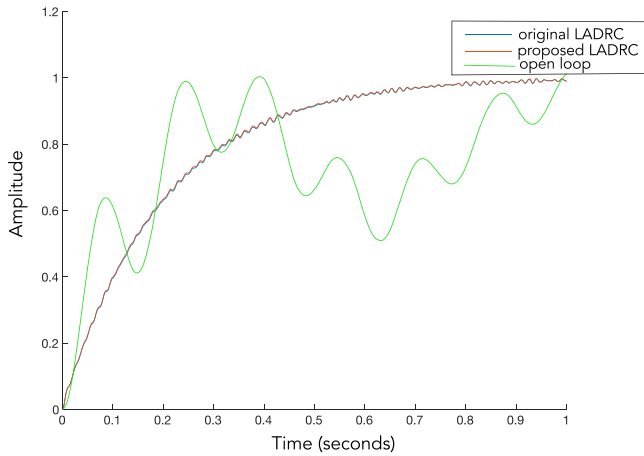

FIGURE 6 Modified LADRC control structure, based on the feedback of the generalized disturbance.

FIGURE 7 Comparison of the disturbance reduction using original LADRC scheme (blue line) and the proposed MLADRC scheme (orange line). The green line shows the disturbance effect at open loop. The open loop gain has been normalized to one, for a better comparison.

FIGURE 8 Delay stability margin, in seconds, depending of the value of the gain K for the system (20).

new scheme is not very different from the original scheme. The obtained advantage is a simpler controller structure, which can be more easily analysed.

In both cases, one of the main features of the proposed GESO is the easy stability analysis as function of the direct loop gain. This is discussed in the next subsection.

Using this novel GESO, a Modified LADRC (MLADRC) structure is proposed, shown in Figure 6. The proposed scheme includes an additional control element, substituting the gain $K = \frac{1}{b}$. Then,

$$e\,(t) = r\,(t) - y_o\,(t)$$
$$u\,(t) = e_f\,(t) \tag{16}$$

where $e_f(t)$ is the output of the transfer function $C(s)$, that is, $E_f(s) = C(s)E(s)$. This element adds flexibility to the designer, which is valid for increasing the delay stability margin of the resulting system. On the other hand, the stability analysis MLADRC (and $C(s)$ design) can be easily performed in the frequency domain, since it only depends on a scalar signal and is applicable with the presence of time delay.

To illustrate the good behaviour of the new MLADRC using $C_o = [0, \ldots, 1]$, it has been applied to the system (13) with $\tau = 0.0001$ s and using $C(s) = \frac{1}{b}$, $b = 1.4$. The MLADRC and the original LADRC have same design parameters: first order, $\omega_o = 1000$ rad/s and $\omega_c = 5$ rad/s. Figure 7 shows the results comparing both LADRC and MLADRC with the open-loop response using a step signal as reference and white noise as input disturbance. The open-loop gain has been normalized to one for better comparison. It can be observed that the disturbance rejection is very good and very similar using both schemes. In this example, the delay τ has been selected low to maintain the system stable without the necessity of a more complex $C(s)$, the system being stable by using the original LADRC.
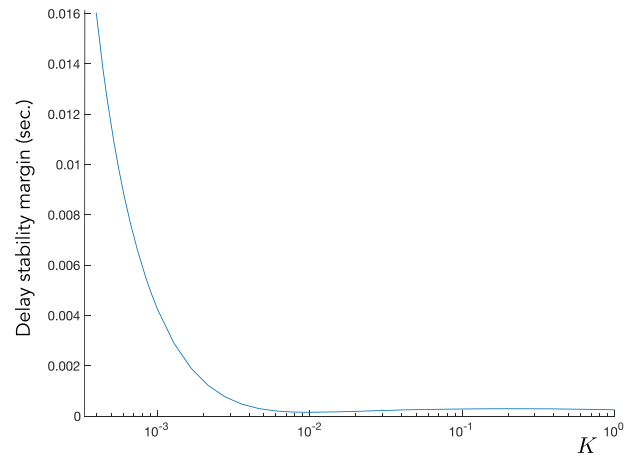
3.1 | Stability analysis of the modified LADRC

Based on the mathematical description of the MLADRC (14), (15), the GESO output can be expressed:

$$Y_o\,(s) = H_{eso}\,(s)\,Y\,(s) + H_{eso}^r\,(s)\,R\,(s)$$
$$H_{eso} = K_o\Big(sI_{(p+1)\times(p+1)} - A_o\Big)^{-1} L_o \tag{17}$$
$$H_{eso}^r = K_o\Big(sI_{(p+1)\times(p+1)} - A_o\Big)^{-1} \frac{B_e}{b}$$

Now, closing the loop with a plant $P(s)$ in the presence of time-delay, the characteristic equation of the MLADRC system is:

$$1 + e^{-\tau s} C\,(s)\,H_{eso}\,(s)\,P\,(s) = 0 \tag{18}$$

with $H_{eso}(s) = C_o(sI - A_o)_o^{-1}L_o$.

Using Equation (18), the stability analysis as a function of the loop gain can be easily performed using the Nyquist criterion. This analysis is especially straightforward when the plant is minimum phase, [21], since the system is stable for a gain that satisfies $K < K_{min}$; that is, if the open loop plant is minimum phase, the system is closed-loop stable for a sufficiently low gain value.

It is important to remark that, in this case, the gain of $C(s)$ is directly related to the reduction of the disturbances and for gain values lower than the value of the matching condition $1/b$, the disturbance reduction is limited.

As an example, the analysis of the system (13) can be used to illustrate the procedure using a first-order MLADRC with $\omega_o = 1000$ rad/s and $\omega_c = 5$ rad/s. Figure 8 shows the delay stability margin of this system choosing $C(s) = K$, as a function of the gain K, obtained from (18). This configuration is equivalent to a classical LADRC controller. As is observed, by reducing the value of the feedback gain, the stability margin improves, but at the cost of losing disturbance reduction. This
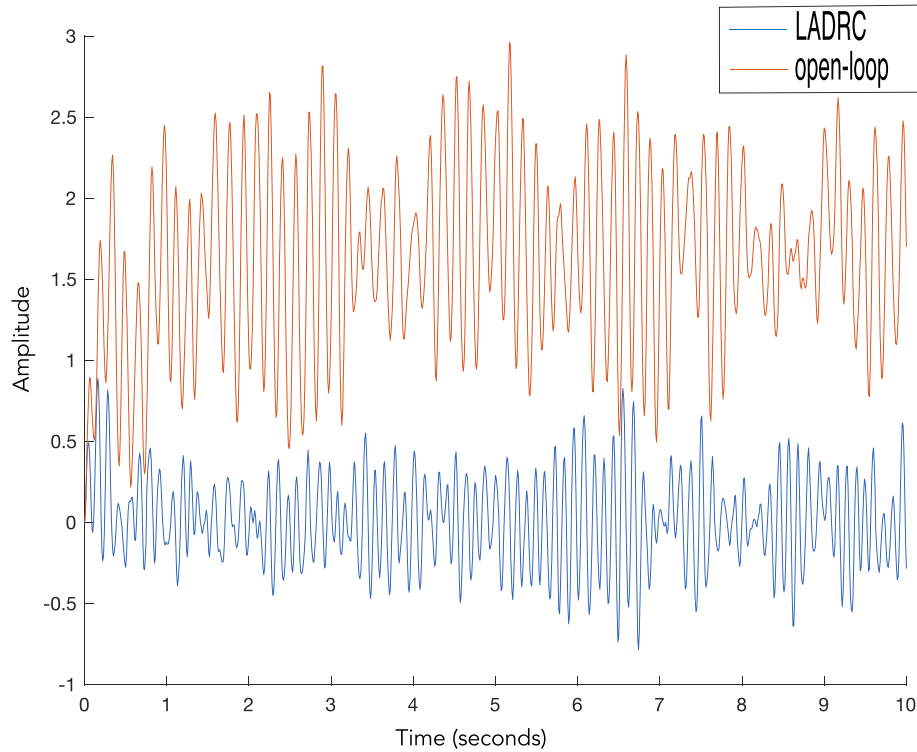
FIGURE 9 Example showing the disturbance response of (18) with a time delay $\tau = 0.001$ s, using $C(s) = K$. A low K value (0.002) is used for maintaining the stability, obtaining a limited disturbance reduction.

fact can be observed in Figure 9. In this case, being the time delay $\tau = 0.001$ s, the gain $K = 0.002$ is chosen from Figure 8 for maintaining the closed loop stability, and a poor disturbance reduction is obtained.

3.2 | Loop shaping design

As the previous example illustrates, gain reduction is a limited design strategy, which may be useful for some systems and with small time-delays. However, the MLADRC presented opens the door to improving the stability by designing $C(s)$, allowing an increment of the loop gain and, as a result, the disturbance reduction. This is one of the main novelties introduced by MLADRC. For instance, the direct gain K can be substituted by a phase compensator, which can be used for shaping the system frequency response.

Loop shaping is a common design methodology which, in fact, can be done following different strategies for obtaining a desired frequency response shape [22]. The controllers can be PIDs, lead or lag phase compensators, notch filters, among others.

In the case of time delayed systems, loop shaping can be applied to compensate the frequency response in the high gain, high phase lag areas. Two possible actions can be introduced: gain reduction or introduction of a lead phase in the critical frequency range. In the case of resonances, lead compensators can be used to improve the phase and notch filters to reduce the system gain in such sensitive frequency ranges. At high frequencies,

a gain-reducing filter can be necessary, as the lag introduced by the delay may be excessive to be able to compensate.

The example (13) presented in the previous sections can be used again to illustrate the procedure, using the same first-order MLADRC with $\omega_o = 1000$ rad/s $\omega_c = 5$ rad/s and the time delay $\tau = 0.001$ s. From Figure 8, the value of the gain should be $K < 2 \times 10^{-3}$ to maintain the system stability. However, the distortion reduction is very poor with such a low gain (see Figure 9).

To increase the gain to a value that gives good disturbance rejection, for instance, $K = 0.3$, a lead compensator is introduced as a direct loop controller $C(s)$. From the Bode diagram of the open-loop system with $K = 0.3$ (Figure 10), the compensator parameters are designed to stabilize the system, obtaining the following transfer function:

$$C(s) = \frac{1 + bT_b s}{1 + T_b s}$$

with $b = 5.8284$ and $T_b = 9.2047 10^{-4}$. This controller increases the phase around the critical frequency of 55 rad/s. Figure 10 shows the Bode diagram of the original open-loop system, with and without delay and the effect of the designed compensator, stabilizing the system. The phase of the MLADRC, the green line, increases from 40 rad/s to 1000 rad/s approximately, thanks to the controller designed $C(s)$, compared with the MLADRC controller using only a constant K. This increment compensates the effect of the delay, increasing the stability margin.
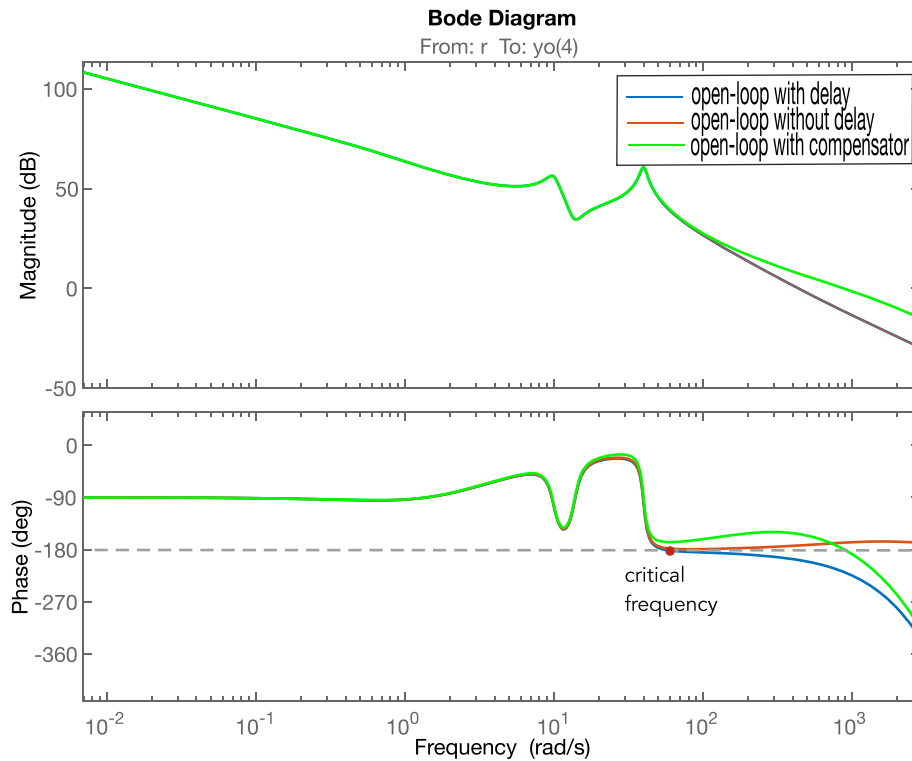
FIGURE 10 Open-loop frequency response comparison, showing the loop shaping effect of the compensator, increasing the phase around the critical frequency: red line, system without delay; blue line, system with delay; green line, system with delay and compensator.
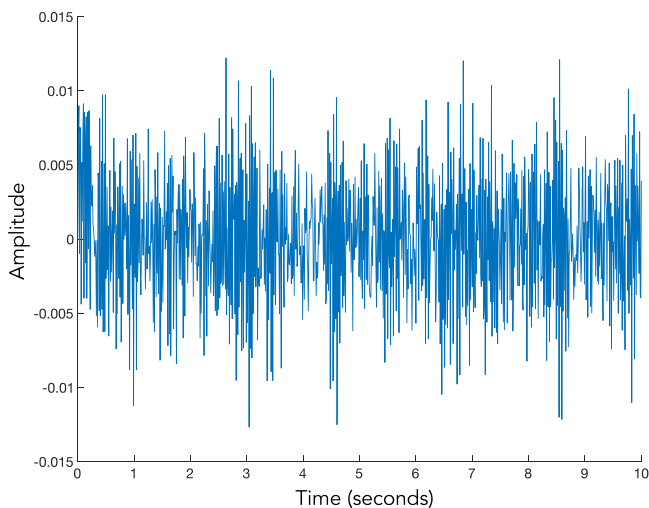

FIGURE 11 Disturbance reduction using the modified LADRC with $K = 0.3$ and a lead compensator for time delay $\tau = 0.001$ s.

Figure 11 shows the disturbance rejection obtained using the gain value $K = 0.3$, thanks to the increased stability margin obtained by the compensator. Note that the input noise is equivalent to the one used in the Figure 9, being the obtained disturbance two orders of magnitude lower. The compensated system is stable for $\tau < 0.0038$ s. To compare performance, using the scheme proposed in [12] and the gain $K = 0.3$, the system becomes unstable for $\tau > 0.00022$ s, that is, the stability margin is one order of magnitude lower.

4 | EXPERIMENTAL VALIDATION

In this section, the aforementioned approach is implemented in a real mechanical system with relevant resonant modes to analyse the feasibility of the design process and the performance of the resulting controller.

4.1 | System description

The mechanical system used to analyse the stabilization process must meet certain characteristics that are important for proper testing of the control algorithm and its ability to reject disturbances. This characteristic is a high sensitivity to mechanical vibrations. This is an added difficulty to control the system and makes a perfect scenario for testing the algorithm, because this type of systems is very sensitive to time-delay, which can become unstable. In this way, the mechanical system selected for this test was a passive flexible structure mounted on a single-axis seismic table for the study of active mass dampers, commercialized by Quanser [23], and shown in Figure 12. The structure has a capacitive accelerometer on its top in order to measure the vibration of the system and is controlled by the linear movement of the shaking table. At the same time, the shaking table is controlled by a high-torque motor connected to it via a rack-and-pinion system. The motor also has a high-resolution optical encoder with which the position of the shaking table is measured. The goal of this implementation is to control the position of the shaking table and the vibration (accelera-
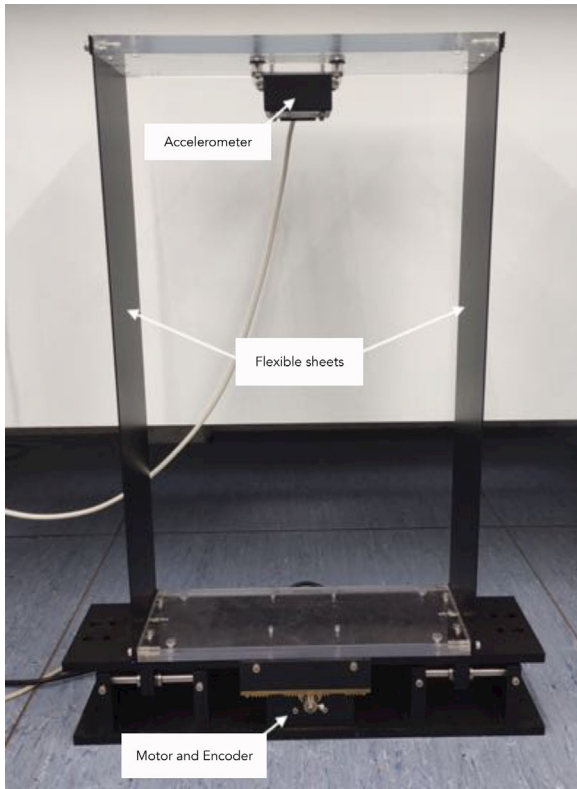
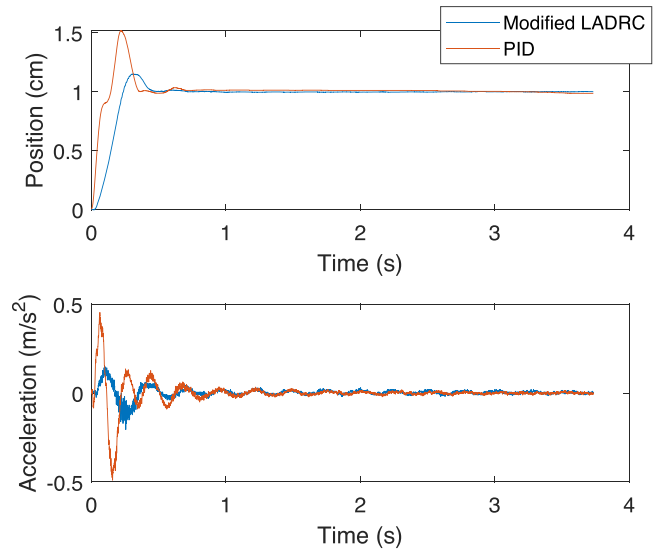**FIGURE 12** Photography of the mechanical system under study.

FIGURE 13 Step response of the system controlled by a well-tuned PID versus the proposed ADRC. The system performance is improved by mean of the MLADRC.

tion) of the top of the structure just by the movement of the motor.

It should be noted that this system has several characteristics that make it highly difficult to control. Firstly, due to the friction that happens in the rack-pinion system and the dead zone of the motor, the system dynamics has a relevant non-linear component. Moreover, due to its geometry, the structure has various relevant resonant modes along the control bandwidth, which make it very sensitive to vibrations. Finally, the objective is to control the top of the structure by moving the table, which is a clear case of a non-collocated control problem.

In order to have a preliminary idea of the dynamics of the system and as a starting point for the design of the loop shaping compensator, a simplified mathematical model of the system in state space have been used, modelling only the most relevant resonant mode, given by the following matrices:

$$
A = \begin{bmatrix} 0 & 0 & 1 & 0 \\ 0 & 0 & 0 & 1 \\ -469.063 & 469.063 & -33.38 & 0 \\ 631.6875 & -631.6875 & 0 & -0.3125 \end{bmatrix}
$$

$$
B = \begin{bmatrix} 0 & 0 & 2.087 & 0 \end{bmatrix}^{T}
$$

$$
C = \begin{bmatrix} 1 & 0 & 0 & 0 \\ 631.6875 & -631.6875 & 0 & -0.3125 \end{bmatrix}
$$

(19)

4.2 | ADRC performance without time-delay

First, the generic performance of the ADRC for the mechanical system given by matrices (19) has been measured. For that purpose, the MLADRC structure described in Figure 6, using Equations (14), (15) was implemented on a myRio device using LabVIEW and its performance was compared with a PID controller tuned by the means of a genetic algorithm based on BLX-alpha crossover [24] (design values, $K_p = 3$, $K_i = 12$, $K_d = 0.006$). The sampling time used in the discrete implementation has been 0.5 milliseconds, thus restricting the ADRC to a maximum bandwidth of 1 KHz.

After extensive testing, it was determined that the second-order MLADRC with a GESO bandwidth of $\omega_o = 250$ Hz and a controller bandwidth of $\omega_c = 15$ Hz is an acceptable compromise between smooth dynamics and good disturbance rejection. In this way, the L_0 and K_0 matrices (15) have been set to place the observer poles at 250 Hz (three poles) and the controller poles at 15 Hz (two poles). As shown in Figure 13, the performance of this an algorithm is superior to that of a PID, because it offers five times less overshoot and much better vibration rejection.

4.3 | Stabilization of the delayed system by loop shaping

To test the proposed stabilization procedure, the control signal has been delayed via software by 5 ms, making the system unstable. Analysing the resulting control signal shown in Figure 14, it can be concluded that the system instability grows in a frequency range around 97 Hz. A compensation around this frequency is necessary in order to maintain the stability, by designing a suitable $C(s)$ controller for the MLADRC (a digital version $C(z)$ in the real implementation).
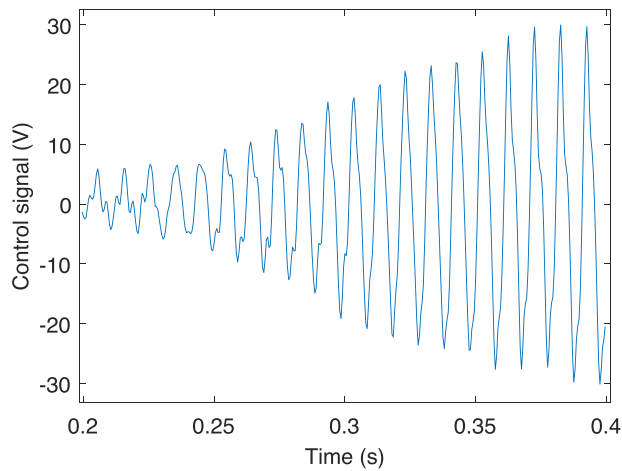
FIGURE 14 Unstable control signal using the MLADCR with $\tau = 0.005$ s and $C(s) = K$, K being a constant gain.
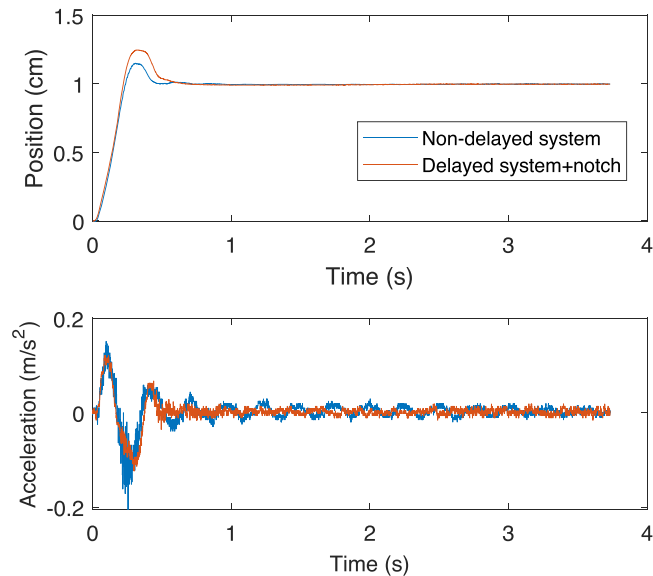

FIGURE 15 Step response of the non-delayed and stabilized systems. Introducing $C = H_{notch}$, the MLADRC is able to compensate the effect of the delay $\tau = 0.005$ s.

In this way, a digital notch filter (20) centred in 97 Hz was implemented as a loop shaping compensator, in order to stabilize the system and improve its dynamics. In this case, the stability is obtained limiting the gain around the critical frequency.

$$H_{notch}(z) = \frac{z^2 - 1.911z + 0.9975}{z^2 - 1.753z + 0.8395} \quad (20)$$

The resulting controller keeps the system step response almost identical (see Figure 15) and improves to a large extent the disturbance rejection (see Figures 15 and 16, respectively), validating the proposed loop shaping-based compensation ADRC scheme.
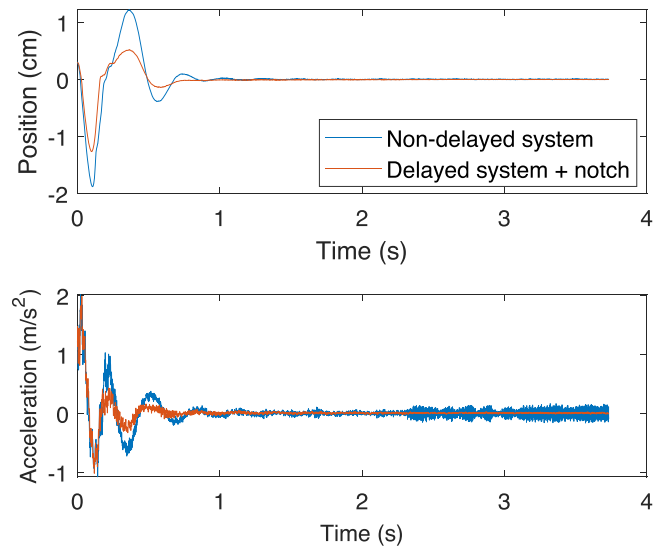

FIGURE 16 External disturbance response of the non-delayed and stabilized systems. Introducing $C = H_{notch}$, the MLADRC is able to compensate the effect of the delay $\tau = 0.005$ s.

5 | CONCLUSIONS

The ADRC algorithm is very effective for disturbance rejection, due to the high gain obtained in the ESO bandwidth. However, this fact makes the ADRC algorithm sensitive to the presence of time delays, since the system can become unstable for relatively low delays. Some algorithms consider this problem, but usually, if stability is improved, disturbance rejection is reduced.

This paper discusses this reduction in stability and its relation to the high gain necessary for good perturbation rejection. The discussion is carried out with systems that include mechanical resonances, where the low relative stability shows clearly the problem, and the disturbance effect is significative for such systems.

For dealing with this problem, a variation of the LADRC controller is presented, the proposed MLADRC scheme, obtaining a simplification of the stability analysis of the algorithm and opening the door to the use of control strategies for improving of the stability range, using additional elements as phase compensators or notch filters. This work proposes the use of an additional controller to achieve a stable system and a good disturbance reduction in the presence of time delay.

An application example using a mechanical system with resonance modes and a non-linear behaviour illustrates the proposed idea, obtaining a significant disturbance reduction improvement, using a loop shaping strategy.

For future works, efforts will focus on testing the MLARDC in practical implementations. In particular, the control scheme will be tested in a superconducting RF cavity for the reduction of microphonic effects, using as actuator a piezoelectric tuner, which presents a small, but significant, time delay. In the tests, different controllers will be implemented for loop-shaping purposes, as lead or lag phase networks, in addition to the notch filters used in this work.

AUTHOR CONTRIBUTIONS

ACKNOWLEDGEMENTS

CONFLICT OF INTEREST STATEMENT

The authors declare no conflicts of interest.

DATA AVAILABILITY STATEMENT

Data available on request from the authors.

ORCID

Josu Jugo https://orcid.org/0000-0003-3935-1513

REFERENCES

1. Han, J.: From PID to active disturbance rejection control. IEEE Trans. Ind. Electron. 56(3), 900–906 (2009)
2. Li, H., Li, S., Lu, J., Qu, Y., Guo, C.: A novel strategy based on linear active disturbance rejection control for harmonic detection and compensation in low voltage AC microgrid. Energies 12(20), 3982 (2019)
3. Zheng, Z.: ADRC control for beam loading and microphonics. In: Proceedings of LINAC2012. Tel-Aviv, Israel, pp. 615–617 (2012)
4. Geng, Z.: Superconducting cavity control and model identification based on active disturbance rejection control. IEEE Trans. Nucl. Sci. 64(3), 951–958 (2017)
5. Huang, Y., Xue, W.: Active disturbance rejection control: Methodology and theoretical analysis. ISA Trans. 53(4), 963–976 (2014)
6. Guo, B.Z., Zhao, Z.: Active disturbance rejection control: Theoretical perspectives. Commun. Inf. Syst. 15, 361–421 (2015)
7. Xiao, J., Li, D., Zhou, J.: Active disturbance rejection controller design for distributed parameter systems. In: 2015 Chinese Automation Congress (CAC). Wuhan, China, pp. 202–207 (2015)
8. Guo, B.Z., Zhao, Z.: Active disturbance rejection control for nonlinear systems: An introduction. Wiley (2016)
9. Sira-Ramirez, H., Luviano-Juárez, A., Ramirez-Neria, M., Zurita-Bustamante, E.: Active disturbance rejection control of dynamic systems: A flatness based approach. Wiley (2018)
10. Neumann, A., Anders, W., Kugeler, O., Knobloch, J.: Analysis and active compensation of microphonics in continuous wave narrow-bandwidth superconducting cavities. Phys. Rev. Spec. Top. Accel. Beams 13, 082001 (2010)
11. Zhao, S., Gao, Z.: Modified active disturbance rejection control for time-delay systems. ISA Trans. 53(4), 882–888 (2014)
12. Zheng, Q., Gao, Z.: On active disturbance rejection for systems with input time-delays and unknown dynamics. In: Proceedings of the 2016 American Control Conference (ACC), pp. 95–100. Boston, USA (2016)
13. Tan, W., Fu, C.: Analysis of active disturbance rejection control for processes with time delay. In: Proceedings of the 2015 American Control Conference (ACC). Chicago, USA, pp. 3962–3967 (2015)
14. Ramirez-Neria, M., Sira-Ramirez, H., Luviano-Juarez, A., Rodriguez-Angeles, A.: Smith predictor based generalized PI control for a class of input delayed nonlinear mechanical systems. In: 2013 European Control Conference. pp. 1292–1297 (2013)
15. Castañeda, L.A., Luviano-Juárez, A., Ochoa-Ortega, G., Chairez, I.: Tracking control of uncertain time delay systems: An ADRC approach. Control Eng. Pract. 78, 97–104 (2018)
16. Fu, C., Tan, W.: Control of unstable processes with time delays via ADRC. ISA Trans. 71, 530–541 (2017)
17. Wu, Z., Li, D., Chen, Y.: Active disturbance rejection control design based on probabilistic robustness for uncertain systems. Ind. Eng. Chem. Res. 9, 59 (2020)
18. Tan, W., Fu, C.: Linear active disturbance-rejection control: Analysis and tuning via IMC. IEEE Trans. Ind. Electron. 63(4), 2350–2359 (2016)
19. Gao, Z.: Scaling and bandwidth-parameterization based controller tuning. In: Proceedings of the 2003 American Control Conference. pp. 4989–4996 (2003)
20. Zhou, R., Tan, W.: A generalized active disturbance rejection control approach for linear systems. In: 2015 IEEE 10th Conference on Industrial Electronics and Applications (ICIEA). pp. 248–255 (2015)
21. Jugo, J.: On the stability of time-delay systems using Nyquist criterion. In: 2001 European Control Conference (ECC). pp. 2717–2722 (2001)
22. Åström, K.J., Murray, R.M.: 'Feedback Systems: An Introduction for Scientists and Engineers. 2nd ed', http://www.cds.caltech.edu/murray/amwiki/Main_Page. Accessed June 2023
23. Quanser. 'Active mass damper', https://www.quanser.com/products/active-mass-damper/. Accessed June 2023
24. Eshelman, L., Schaffer, J.: Real-coded genetic algorithm and interval-schemata. Found. Genet. Algorithms 2, 187–202 (1993)